

# Manipulation of One-Dimension Photonic Crystal Spectrum via Perforated Silicon Slab

Borys Chernyshov\* and Sergei I. Tarapov

**Abstract**—This paper describes the study of zone-spectra of one-dimension finite-element photonic crystal quartz/silicon in the millimetre waveband. The silicon elements of photonic crystal are performed as slabs with holes. The numerical and experimental investigations have demonstrated the possibility of using the effective medium approach for the silicon element of photonic crystal. The paper introduces a simple phenomenological formula for the calculation of effective permittivity of perforated silicon slab.

## 1. INTRODUCTION

As known, a photonic crystal is a structure in which the refractive index changes spatially and periodically [1]. The major property of photonic crystals spectra is the existence of allowed and forbidden bands of electromagnetic wave propagation. Such a structure of photonic crystals spectra is similar to the structure of electron energy spectra in solids. The properties of photonic crystals allow them to be widely used as frequency filters, lasers, waveguides with low losses, and as the key elements in optical computers [2]. It is widely known that 1D, 2D, 3D photonic crystals consist of dielectric layers [3]. The dielectric photonic crystals might be used in different frequency ranges including millimetre range. A downside to dielectric photonic crystals is that it is impossible to manipulate the spectrum band structure. There are many papers devoted to creating and controlling the photonic crystal spectra using ferrites [4]. The presence of ferrites in photonic crystals permits to change the photonic band gap by using the external permanent magnetic field. Unfortunately, to reach a sufficiently large shift of band gap, it is necessary to apply a very large magnetic field (about 1kOe), so we cannot talk about the efficient control of photonic band gap; and very large magnets would be required in any case. For this reason, the actual problem is controlling the photonic band gap using the external electric field or electromagnetic radiation instead of magnetic field. Semiconductor materials seem to be a promising option for addressing this problem [5]. The use of these materials allows for varying the spectrum of photonic crystal using the electromagnetic radiation, temperature or external bias voltage. However, in the millimetre waveband, the losses in the semiconductor are very large and almost all energy of electromagnetic wave is absorbed by the sample. To be able to use semiconductors in the microwave range, these losses need to be reduced significantly. There are different ways to address this problem: by, for example, using donor or acceptor dopes [6], low temperatures [7]. A possible way to reduce the effect of losses in semiconductor is to structure the surface by perforating holes in a semiconductor slab. But in this case, the continuous medium condition for all ( $d \ll \lambda$ ) is not obvious. If so, every hole in the sample must be considered as a separate element which is quite a difficult task.

The aim of this paper is to consider the use of a continuous medium model by examining the transmission of electromagnetic waves through the perforated silicon slabs, which are the elements of the photonic crystal.

---

*Received 22 July 2016, Accepted 14 September 2016, Scheduled 30 September 2016*

\* Corresponding author: Borys Chernyshov (boris.chernyshev@gmail.com).

The authors are with the Radiospectroscopy Department, O.Ya. Usikov Institute for Radiophysics and Electronics of NASU, 12 Ak. Proskura Str., Kharkiv 61085, Ukraine.

## 2. DESCRIPTION OF THE STRUCTURE, MOTION EQUATIONS

One-dimension finite-element photonic crystal (PC) consisting of 8 unit cells from quartz and silicon (Fig. 1) is under investigation. The PC is constructed using slabs whose linear dimensions are  $a \times b = 7.2 \times 3.4$  mm (the experimental implementation is shown in Fig. 4). The permittivity of quartz is assumed as  $\varepsilon_1 = 3.8$ , and its width is  $d_1 = 2$  mm. The width of the silicon layer equals  $d_2 = 0.34$  mm. The holes with a diameter of  $d = 0.5$  were fabricated in the silicon. These holes are located on the slab in different geometrical configurations: “5 × 3”; “6 × 4”; and “7 × 5” (Fig. 2). In the first configuration, fifteen holes are located five in three rows. The second configuration comprises twenty four holes located six in four rows. In the third configuration, thirty five holes are located seven in five rows. To describe the complex permittivity of silicon, we use the known Drude model [8]:

$$\varepsilon_2 = \varepsilon_p \left[ 1 - \frac{\omega_{pn}^2}{\omega(\omega + i\nu_n)} - \frac{\omega_{pp}^2}{\omega(\omega + i\nu_p)} \right], \quad (1)$$

where  $\omega_{pn}$ ,  $\omega_{pp}$  are plasma frequencies of electrons and holes in semiconductor;  $\nu_n$ ,  $\nu_p$  are electrons and holes collision frequencies;  $\varepsilon_p = 11$ , 8 is the lattice part of permittivity in silicon;  $\omega$  is the frequency of the incident electromagnetic wave.

The expression for the plasma frequency is given by [10]:

$$\omega_{pn,p} = \sqrt{4\pi e^2 n_{n,p} / m_{n,p}^* \varepsilon_p}, \quad (2)$$

where  $n_{n,p}$  are electrons and holes concentrations respectively;  $m_{n,p}^*$  are effective masses of charge carriers;  $e$  is the electron charge.

The collision frequencies of charge carriers are coupled with carrier mobility and can be determined using the relation [9]:

$$\nu_{n,p} = e / \mu_{n,p} m_{n,p}^*, \quad (3)$$

where  $\mu_{n,p}$  is the electrons and holes mobility.



**Figure 1.** Dielectric photonic crystal: 1 — quartz layer with the thickness  $d_1$ , 2 — silicon layer with the thickness  $d_2$ .

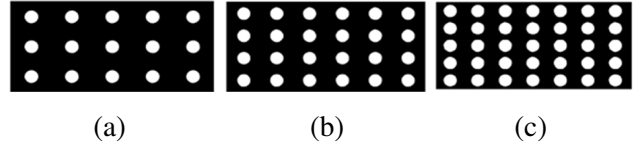


**Figure 2.** Location of holes in silicon slab: (a) “5 × 3”; (b) “6 × 4”; (c) “7 × 5”.

The electron and hole concentration values are coupled with the intrinsic carrier concentration in the relation:  $n_i^2 = n_n n_p$  [11]. The intrinsic concentration value for silicon under room temperature is  $n_i = 1 \cdot 10^{10}$  cm<sup>-3</sup>. The charge carrier mobility values are as follows:  $\mu_n = 1400$  cm<sup>2</sup>/(V·s),  $\mu_p = 500$  cm<sup>2</sup>/(V·s). The charge carrier effective masses are equal to  $m_n^* = 0.98m_0$ ;  $m_p^* = 0.49m_0$ , where  $m_0$  is the mass of free electron.

Note that a similar structure made of metallic film with sub-wavelength holes dimensions was considered in [12]. That paper shows that in metallic film with holes the abnormal transparency arises due to the resonance interaction of surface plasmons with incident electromagnetic wave. Our paper does not address the excitation of surface plasmons because the real part of silicon permittivity that is under investigation here for the considered frequency range is positive. In this case, the surface electromagnetic waves in the considered structure do not exist. Besides, there are papers in which not metallic but semiconductor structure with holes is under investigation [13] where the holes in semiconductor film are regarded as a photonic crystal. Disorder of position holes in the semiconductor film lead to the generation of electromagnetic modes coupled with Anderson localization. In our paper, the semiconductor slab with holes is not considered as a photonic crystal.

The most common models for describing the averaged medium permittivity with positive real part are Maxwell-Garnett's model [14] and Bruggeman's model [15]. These models are used for electromagnetic description of media with spherical inclusions having dimensions well below the wavelength. Note, however, that these models have a complicated form when describing medium with permittivity as Eq. (1). In addition, in the structure considered in our paper, the inclusions have a cylindrical form. In a thin slab approximation, these inclusions are circular, so they might hardly be viewed as polarizing centres on which the Maxwell-Garnett and Bruggeman's models are based.

We use a simple phenomenological formula for describing a silicon structure with holes in it. Our formula uses the Drude formula as a basis in Eq. (1). In that formula, we introduce the fill factor coefficient for holes in silicon slab. In this case, the form and location of holes are not taken into account. The formula that we consider appears as follows:

$$\varepsilon_{eff} = \varepsilon_2 (1 - \delta), \quad (4)$$

where  $\delta = V_1/V_2$  is the fill factor coefficient of silicon slab,  $V_1$  the total volume of all holes in the slab, and  $V_2$  the total slab volume.

In the case when the holes have a cylindrical form, and the slab is a rectangular parallelepiped. The fill factor coefficient of silicon slab should be calculated as a ratio between the surface areas of all holes and entire slab.

To calculate the transmission coefficients, we use the transmission matrix technique [16] and FDTD-technique. The FDTD-technique has been realized by using CST Microwave Studio Suite Student Edition. The transmission matrix for unit cell of the considered photonic crystal is given by:

$$M = \begin{pmatrix} M_{11} & M_{12} \\ M_{21} & M_{22} \end{pmatrix}, \quad (5)$$

where  $M_{11} = \cos(k_1 d_1) \cos(k_2 d_2) - (n_2/n_1) \sin(k_1 d_1) \sin(k_2 d_2)$ ;  $M_{12} = -i[(1/n_2) \cos(k_1 d_1) \sin(k_2 d_2) + (1/n_1) \sin(k_1 d_1) \cos(k_2 d_2)]$ ;  $M_{21} = -i[n_1 \sin(k_1 d_1) \cos(k_2 d_2) + n_2 \cos(k_1 d_1) \sin(k_2 d_2)]$ ;  $M_{22} = \cos(k_1 d_1) \cos(k_2 d_2) - (n_1/n_2) \sin(k_1 d_1) \sin(k_2 d_2)$ .

The transmission matrix for all photonic crystals from 8 unit cells is given by  $m = M^8$ . The transmission coefficient is defined as:  $T = |t^2|$ , where  $t = 2/(m_{11} + m_{12} + m_{21} + m_{22})$ .

The refractive indexes are determined as  $n_{1,2} = \sqrt{\varepsilon_{1,2}}$  — in the case when a slab has no holes and when there is no slab (thereat  $\varepsilon_2 = 1$  is the permittivity of air). In the case when a slab with holes is used, the substitution  $\varepsilon_2 \rightarrow \varepsilon_{eff}$  takes place. Because the materials are non-magnetic, the permeability equals 1 and does not affect the refractive indexes. The wavenumbers are defined as  $k_{1,2} = \sqrt{(\omega/c)^2 n_{1,2}^2 - k_x^2}$ , where  $c$  is the light velocity in vacuum, and  $k_x = \pi/a$  is the transverse wavenumber in which  $a$  is the length of a long wall of waveguide. In our paper, the electron silicon KEF-100 with electrons concentration  $n_n = 2 \cdot 10^{13} \text{ cm}^{-3}$  is under investigation. The fill factor coefficient of silicon slab with holes for different structures equals 0.125 for structure “5 × 3”; 0.19 for structure “6 × 4”; and 0.28 for structure “7 × 5”. We also calculated two boundary cases: 1) silicon slabs are regarded complete (“Full” in Fig. 3), and 2) there are not silicon slabs (photonic crystal quartz/air). The results of calculations of transmission coefficient in the frequency range 0–120 GHz are presented in Figs. 3(a), (b). In order to find a more effective way for calculating spectra, the following two methods were employed: FDTD-technique and transmission matrix technique. In these figures, the minimum values of transmission coefficients correspond to forbidden bands and maximum values correspond to allowed bands. As can be seen, the fill factor coefficients corresponding to the forbidden bands shift towards the higher frequencies as the number of holes in the silicon slab increases. At the same time, the minimum values of transmission coefficients decrease, and their widths shrink by about 10%. It can also be seen that the left edge of a forbidden band shifts more than the right edge.

The observed effect is explained by a change in the effective dielectric permittivity of slab caused by a change in the fill factor coefficient of holes in the silicon slab.

It can be seen that the graphs in Fig. 3(a) and Fig. 3(b) have some differences with respect to the minimum values that are less deep in Fig. 3(a). There is also an insignificant difference in the forbidden bands widths.

The discrepancy in minimum values of transmission coefficients calculated using the FDTD and matrix techniques is caused by the following factors: when using FDTD-technique, the calculating

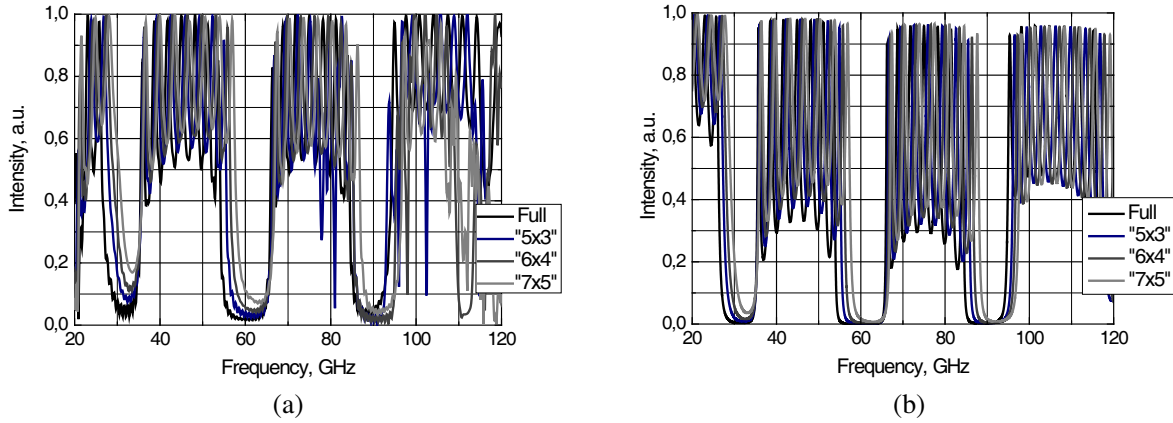


**Figure 3.** Numerical calculations of band structure spectra of photonic crystals with silicon slabs: (a) FDTD-method; (b) transmission matrix method.

structure splits into tetrahedral cells. So this method allows to take into account the geometrical parameters of the structure with a good precision about 0.01 mm (0.08 wavelength). In matrix technique, we use the average, and this obviously means lower precision. Definitely, the FDTD-technique is much more accurate. But the calculation process takes much more time (for comparison, the calculation process is about half a minute with the matrix technique and about 5 minutes with the FDTD-technique). The FDTD-technique also requires special software while the matrix technique does not.

### 3. DESCRIPTION OF THE EXPERIMENT

We inserted the photonic crystal comprising 8 unit cells from quartz and silicon layers in the measuring cell using the technique described in [5]. The measuring cell is fitted to ports of Vector Network Analyzer VNA Agilent PNA-L N5230 A. The measurement is carried out in the frequency range 22–40 GHz.

For the experiment, we used silicon slabs with holes of two configurations “ $5 \times 3$ ” & “ $6 \times 4$ ” to form the photonic crystal (Fig. 4 (2, 3, 4)). The holes with a diameter of 0.5 mm were fabricated using laser technology. The slab of configuration “ $7 \times 5$ ” was impossible to fabricate because of greater fragility and shifting the holes toward the edge of the slab under bleaching. These slabs were therefore not considered in the experiment.

The observed spectra are presented in Figs. 5(a), (b). The spectrum of photonic crystal formed by slabs with “ $5 \times 3$ ” holes is much more precise than the spectrum of photonic crystal formed of slabs with “ $6 \times 4$ ” holes. The absorption values in the forbidden band are about 18 dB. At the same time,

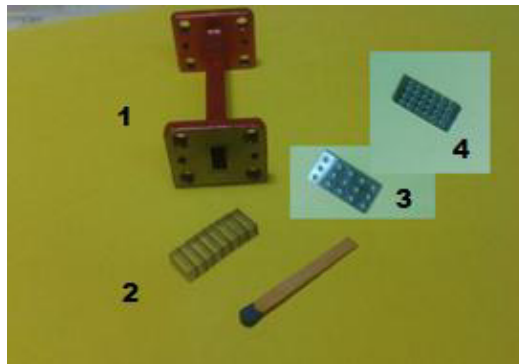


**Figure 4.** Measuring cell (1) and photonic crystal quartz/silicon (2); insert silicon slabs “ $5 \times 3$ ” (3) and “ $6 \times 4$ ” (4).

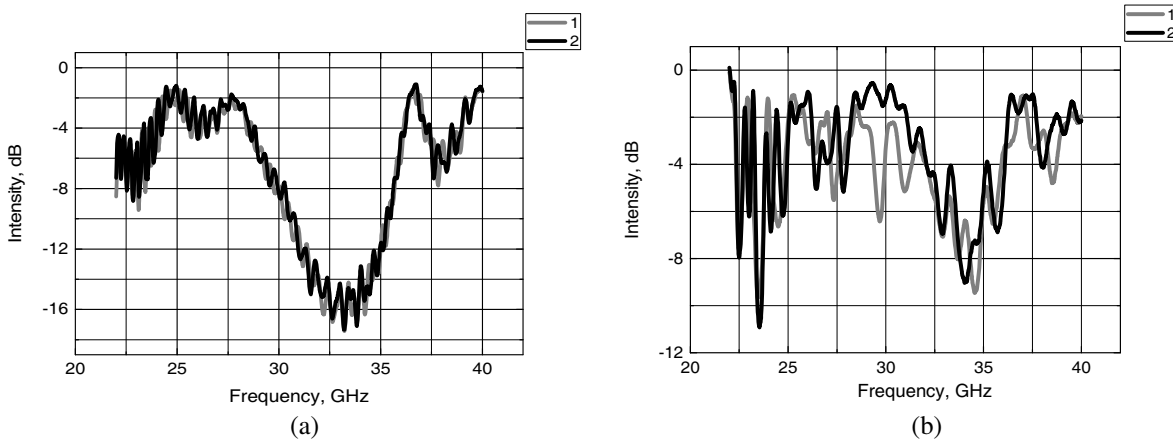


**Figure 5.** Experimental transmission spectra of photonic crystals: (a) with slabs “ $5 \times 3$ ”; (b) with slabs “ $6 \times 4$ ”.

the absorption values in the forbidden band of photonic crystal formed of slabs with “ $6 \times 4$ ” holes do not exceed 10 dB, and there are blips in the spectrum. It is likely to be associated with a large area of oxide film that has been developed due to holes bleaching and possible cracks and cleavages of slabs.

#### 4. RESULTS AND DISCUSSION

To analyse the results, a graph of dependence of left and right edges of forbidden bands upon the fill factor coefficient of holes in the silicon slab has been plotted. On the graph (Fig. 6), the numerical (matrix technique and FDTD-technique) and experimental results are presented. One can see from Fig. 6 that the dependence of the left edges of forbidden band upon the fill factor coefficient of holes in the silicon slab has a similar form. The left edge of the forbidden band frequency calculated using the FDTD-technique is about 1 GHz higher than that calculated using the transmission matrix technique. In the experiment, the frequency of the left edge of forbidden band is about 2 GHz higher than that was calculated by the transmission matrix technique. Thus, the quantitative discrepancy of the numerical and experimental results is less than 10%. For the right edge of the forbidden band, the quantitative consistency of numerical and experimental results is even better. It should be noted that the difference between the numerical calculations produced using two above mentioned algorithms is practically imperceptible, being less than 1%. The experimental values differ from the numerical estimates by less than 1 GHz (about 3%). The experiment shows quite good agreement with the numerical calculations, so we can talk about the applicability of continuous medium model for photonic crystal that has been considered in this paper.

The discrepancies in results are most likely caused by the shortcomings in the silicon slabs with configuration “ $6 \times 4$ ”, such as cracks and cleavages (experimental data for photonic crystal from slabs of this configuration type are less consistent with results of numerical calculations than those for photonic crystal from slabs with configuration type “ $5 \times 3$ ”, Figs. 5(a), (b)). Furthermore, our model does not take into account the development of the oxide film on the silicon surface. It might be important because the oxide film with holes on the slab type “ $6 \times 4$ ” occupies most of the surface space in contrast to the slab type “ $5 \times 3$ ”. This fact may lead to re-reflections, local deviations in periodicity and deterioration of electromagnetic wave dumping in photonic crystal constructed of slabs of “ $6 \times 4$ ” configuration.

A quite good agreement between the calculations and experimental result suggests the possibility of using the continuous medium approach for describing the spectrum of photonic crystal quartz/silicon with holes in silicon whose dimensions can be large enough and even within the order of wavelength. The qualitative and quantitative comparison of results demonstrates the possibility of using the simple formula for estimating the effective permittivity of the perforated silicon slab in the millimetre waveband. Moreover, this approach permits not to take into account the form and location of imperfections and also not to consider them as polarizing centres.

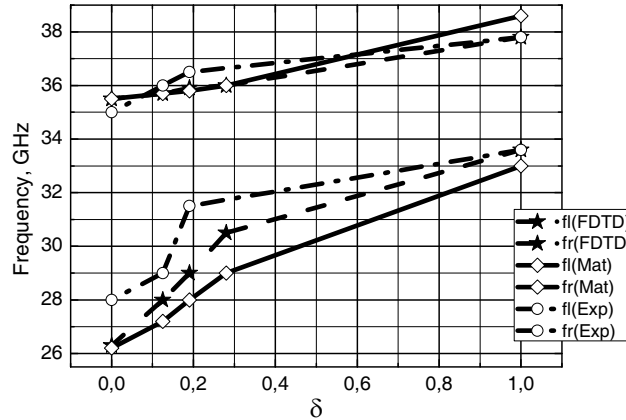


**Figure 6.** The dependence of left edge frequency ( $f_l$ ) and right edge frequency ( $f_r$ ) of forbidden band upon the fill factor coefficient of holes in silicon ( $\delta$ ): FDTD method; matrix method (Mat); experiment (Exp).

## 5. CONCLUSIONS

The numerical and experimental investigations of one-dimension finite-element photonic crystal quartz/silicon containing silicon slabs with holes whose dimensions are within the order of wavelength has been carried out in the microwave range. A simple formula for calculating the effective permittivity of perforated slabs which takes into account holes in silicon slab fill factor coefficient has been introduced and verified. The experimental data show a quite good agreement with numerical calculation results of spectrum of photonic crystal. The divergence between the numerical calculations and experimental results is less than 10%. This small divergence confirms that the proposed formula well describes the spectrum of photonic crystal quartz/silicon with holes whose dimensions are in the order of wavelength.

## ACKNOWLEDGMENT

The authors thank the Materials for Electronics and Solar Cells Department of the National Technical University “Kharkiv Polytechnic Institute” for providing the silicon KEF-100 single crystal and the ALTLASER company staff for providing the laser engraving services required to produce the samples.

## REFERENCES

1. Yablonovitch, E., “Inhibited spontaneous emission in solid-state physics and electronics,” *Physical Review Letters*, Vol. 58, No. 20, 2059–2062, 1987.
2. Lin, S. Y., “Photonic band gap quantum well and quantum box structures: A high-Q resonant cavity,” *Applied Physics Letters*, Vol. 68, 3233–3235, 1996.
3. Joannopoulos, J. D., R. D. Meade, and J. N. Winn, *Photonic Crystals: Molding the Flow of Light*, 54–93, Princeton University Press, 1995.
4. Chernovtsev, S. V., D. P. Belozorov, and S. I. Tarapov, “Magnetically controllable 1D magnetophotonic crystal in millimeter wavelength band,” *J. Phys. D: Appl. Phys.*, Vol. 40, 295–299, 2007.
5. Tarapov, S. I., D. P. Belozorov, “Microwaves in dispersive magnetic composite media (review article),” *Low Temperature Physics*, Vol. 38, No. 7, 766–792, 2012.
6. Chernyshov, B., “Influence of charge carrier density in silicon on spectrum band structure of photonic crystal,” *International Young Scientists Forum on Applied Physics*, 2015, doi: 10.1109/YSF.2015.7333188.

7. Bulgakov, A. A. and V. K. Kononenko, "Slow waves in a periodic structure with a magnetically active semiconductor layers," *Radiophysics and Electronics*, Vol. 2(16), No. 2, 63–70, 2011 (in Russian).
8. Animalu, A., *Intermediate Quantum Theory of Crystalline Solids*, 264–266, Prentice-Hall, Inc., New Jersey, Englewood Cliffs, 1977.
9. Anselm, A. I., *Introduction in Semiconductors Theory*, 328–332, Physnathgiz, Leningrad, 1962 (in Russian).
10. Achiezer, A. I., I. A. Achiezer, R. V. Polovin, A. G. Sitenko, and K. N. Stepanov, *Electrodynamics of Plasma*, 18–24, Nauka, Moscow, 1974.
11. Seeger, K., *Semiconductor Physics*, 23–28, Springer-Verlag, Wien/New York, 1973.
12. Ebbesen, T. W., H. J. Lezak, H. F. Ghaemi, T. Thio, and P. A. Wolff, "Extraordinary optical transmission through sub-wavelength hole arrays," *Nature*, Vol. 391, 667–669, 1998.
13. Sapienza, L., H. Thyrrerstrup, S. Stobbe, P. D. Garcia, S. Smolka, and P. Lodahl, "Cavity quantum electrodynamics with anderson-localized modes," *Science*, Vol. 327, 1352–1355, 2010.
14. Garnett, J. C. M., "Colours in metal glasses and in metallic films," *Phil. Trans. R. Soc.*, Vol. 203, 385–420, London, Ser. B., 1904.
15. Bruggeman, D. A. G., *Ann. Phys. Leipzig*, Vol. 24, 636–664, 1935.
16. Born, M. and E. Wolf, *Principles of Optics: Electromagnetic Theory of Propagation, Interference and Diffraction of Light*, 77–96, Frankfurt, Pergamon Press, Oxford, London, Edinburgh, New York, Paris, 1964.